

SIMULATION OF SURFACE RUNOFF FLOW IN A MODEL URBAN CATCHMENT USING A PARTICLE METHOD

Akihiko Nakayama Xin Yan Lye

ABSTRACT

The Weakly Compressible Smoothed Particle Hydrodynamics (WCSPH) method which was previously applied to rainfall-runoff simulation on natural topography has been reformulated to enable simulation of the rainfall runoff on urban terrain with array of buildings. The reformulation indicates the basic equations of the original WCSPH may be used but suggest more logical modeling of the dynamics as the interaction with neighboring fluid, the ground solid bodies. The simulation of overland flow due to rainfall on an urban terrain with model buildings is successfully conducted and the method is found to represent three-dimensional flow correctly. Unlike depth-averaged flow analyses the water depth is not the main variable in the governing equation but can be obtained by a separate post processing that considers the relation of the real water depth and the distribution of lumps of water for which the governing equations are applied.

1. INTRODUCTION

As the global climate continues changing, forecasting and predicting rainfall runoffs and possible inundation and flooding due to unexperienced rainfalls are becoming very important. The existing methods and models used in rainfall runoff analyses are mostly based on the two-dimensional analyses of Shallow-Water Equations (SWE) (e.g. Zhang and Cundy¹⁾, Teng et al.²⁾, Li et al.³⁾, Constabile et al.⁴⁾, Sayama et al.⁵⁾). They are physical simulation of overland flows given the rainfall hyetographs on specific terrain geometry and are more realistic than more common data-driven models that use statistical correlations between rainfalls and the runoff hydrographs of the past events (e.g. Sitterson, et al.⁶⁾, Gayathri, et al.⁷⁾, Kokkonen, et al.⁸⁾). However, there still are limitations associated with the Eulerian grid-based models that assume hydrostatic pressure distribution. The surface flows that occur due to rainfalls on modern urban areas with structures and buildings present challenges due to their highly three-dimensional features that existing surface flow analysis methods.

In recent years, in contrast to the fixed grid methods, the Smoothed Particle Hydrodynamics (SPH) method developed for analysis of three dimensional free-surface flows has also been applied to the analysis of overland flows due to rainfalls (Chang et al.⁹⁾, Fei et al.¹⁰⁾). The SPH method are a little more flexible but in these 2-d SPH methods, surface water is represented by discrete columns of water of varying depths. The horizontal velocity and the height of these columns are then calculated by the SWE with the SPH method. The rainfall onto ground surface and infiltration into subsurface are modelled by increasing or decreasing the column height. While these methods are numerically efficient, the dynamics of the motion of water is within the framework of shallow water approximation with hydrostatic pressure and additional 1-d analysis of stream flows, if they exist, need to be implemented. These meshless particle interpolation methods have great potential in representing the rainfall itself and the subsequent motion on and in the ground. The 2-dimensional version has been extensively developed and used in overland flow analysis^{9,10,11)}. However they are still limited to the surface flow only and the flows in channels where the shallow surface need to be analyzed separately by 1-d channel flow analysis⁹⁾.

The 3-d SPH method^{12,13)} on the other hand has been shown to represent the motion of sparsely distributed surface flows as well as ponded patches of water and the channel flows at the same time. The present authors have proposed such method and applied to simulation of the rainfall runoff in a small catchment^{14,15)}. In that work, though the runoff in a real urban area from mountainous catchment was simulated successfully, quantitative validation with either measured or observed runoff was not done. In the present work the method is further extended to improve the surface roughness effects and applied to the case of runoff in a model urban catchment for which experimental data on the discharge runoff are available. Also simulation using existing methods has been done and the results with the present new method may be compared. Therefore, the present results are compared with the experimental data and analysis done by SWE analysis and the applicability and the accuracies are examined.

2. SMOOTHED PARTICLE METHOD FOR OVERLAND FLOW DUE TO RAINFALL IN NATURAL AND URBAN TERRAIN

2.1 Basic equations of 3d-SPH method

The conventional methods of rainfall runoff simulation start with the shallow-water approximation of free surface flow on ground. They solve for the depth-averaged flow velocities assuming the hydrostatic pressure assumption. They are effective when the overland flow is spread over mild terrain surface. When the terrain varies rapidly or when there are large buildings, the flow falling on the three-dimensional topography cannot be represented well by these models. Approximations such as the ‘building hole’ or ‘building block’ are used when the effects of buildings are not negligible (Constabile et al.⁴⁾), but they cannot represent rain falling from structures roofs. Particle methods such the basic SPH method on the other hand can cope with these three dimensional effects (e.g. Monaghan¹²⁾). But in the simulation of shallow and patchy overland flow correct representation of the ground roughness is important. The present formulation models the effective depth of shallow flow in order to represent the ground friction accurately. A typical water distribution during or after a rainfall is like that shown in Fig. 1. The ground is mostly dry with thin overland flow, some areas of ponded water and possible nearby streams and watercourse where the flow can be deep and three-dimensional. Therefore, we represent the water as a collection of lumps of water of finite sizes (Fig.2) and formulate the basic equations for them. The size of the lumps determines the resolution of the simulation but the actual patches or drops of water cannot be resolved in full.

We formulate the equations of motion for a water lump a of material volume Ω_a centered at position ra in terms of the density ρ_a and the velocity v_a defined by the volume integral

$$\rho_a = \frac{m_a}{V_a} = \frac{1}{V_a} \int_{\Omega_a} \rho dV \quad \text{and} \quad v_a = \frac{1}{m_a} \int_{\Omega_a} \rho v dV \quad (1)$$

where m_a and V_a are the mass and the volume of lump a . m_a is constant because Ω_a is a material volume and the mass is

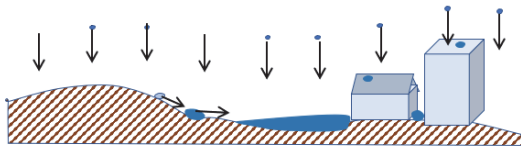


Fig.1 Model terrain and surface water.

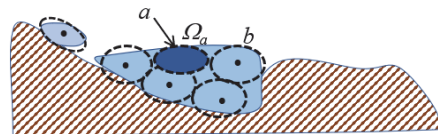


Fig.2 discretization of overland flow by water lumps

conserved. The continuity and momentum equations can be written as the material derivative of ρ_a and \mathbf{v}_a as

$$\frac{d\rho_a}{dt} = -\frac{\rho_a}{V_a} \int_{\partial\Omega_a} \mathbf{v} \cdot \mathbf{n} dS \quad (2)$$

$$m_a \frac{d\mathbf{v}_a}{dt} = \frac{d}{dt} \int_{\Omega_a} \rho \mathbf{v} dV = \int_{\Omega_a} \rho \mathbf{g} dV + \int_{\partial\Omega_a} \mathbf{f}_s dS = m_a \mathbf{g} + \int_{\partial\Omega_a} \mathbf{f}_s dS \quad (3)$$

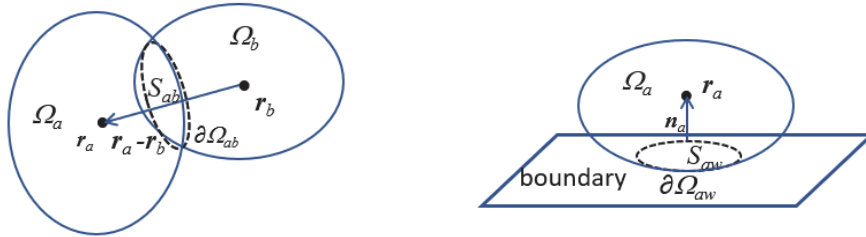
where $\partial\Omega_a$ is the surface enclosing Ω_a , and \mathbf{n} is the unit normal vector on $\partial\Omega_a$.

Therefore, if the volume flux and the surface force on the surface surrounding are evaluated these equations allow time evolution of ρ_a and \mathbf{v}_a . Ω_a is the sum of the interface between lump a and its neighboring lumps b and the surface facing the boundary (Fig.3). These surface integrals can then be approximated by the sum of surface contributions

$$\int_{\partial\Omega_a} \mathbf{v} \cdot \mathbf{n} dS = \sum_b \mathbf{v}_{ab} \cdot \frac{\mathbf{r}_a - \mathbf{r}_b}{|\mathbf{r}_a - \mathbf{r}_b|} S_{ab} + v_n S_{aw} \quad (4)$$

$$\int_{\partial\Omega_a} \mathbf{f}_s dS = \sum_b p_{ab} \cdot \frac{\mathbf{r}_a - \mathbf{r}_b}{|\mathbf{r}_a - \mathbf{r}_b|} S_{ab} + \sum_b \mu_{ab} \frac{\mathbf{v}_a - \mathbf{v}_b}{|\mathbf{r}_a - \mathbf{r}_b|} S_{ab} + \mathbf{T}_w \quad (5)$$

where the summation is taken over the neighboring particles b that are within the influence distance h of 2.3 times the size of the lump, \mathbf{v}_{ab} is the velocity on the interface between lump a and b relative to the velocity of lump a , v_n is the normal velocity on the boundary surface if it is within the influence distance h , S_{ab} and S_{aw} are the area of the interface between lumps a and b and between a and the boundary, respectively, P_{ab} is the pressure force due to particle b , μ_{ab} is the effective viscosity due to particle b and \mathbf{T}_w is the force due to the solid boundary. Note that $\frac{\mathbf{r}_a - \mathbf{r}_b}{|\mathbf{r}_a - \mathbf{r}_b|}$ is the unit vector in the direction from lump b to lump a .



(a) Interaction between neighboring lumps

(b) Interaction between lump a and boundary

Fig. 3 Interface between water lumps a and b (a) and between water lump a and the boundary (b).

The forms of \mathbf{v}_{ab} , P_{ab} and μ_{ab} depend on the exact positions and orientations of the lumps a and b , but if they are taken similar to the form used for continuous flow and

$$\mathbf{v}_{ab} = \frac{1}{2}(\mathbf{v}_b - \mathbf{v}_a) \quad (6)$$

$$P_{ab} S_{ab} = \left(\frac{p_a}{\rho_a} + \frac{p_b}{\rho_b} \right) \frac{m_b}{\rho_b} \nabla_a W_{ab} \quad (7)$$

$$\mu_{ab}S_{ab} = \frac{m_b}{\rho_b} \left(\frac{(\mu_a + \mu_{Ta}) + (\mu_b + \mu_{Tb})}{\rho_b \rho_b} \right) (\mathbf{v}_a - \mathbf{v}_b) \frac{(\mathbf{r}_a - \mathbf{r}_b)}{|\mathbf{r}_a - \mathbf{r}_b|^2} \cdot \nabla_a W_{ab} \quad (8)$$

where p_a and p_b are the pressure, ρ_a and ρ_b are the density, μ_a and μ_b are the molecular viscosity, μ_{Ta} and μ_{Tb} are the turbulent viscosity, \mathbf{r}_a and \mathbf{r}_b are the positions of particles a and b , respectively, m_b is the mass of particle b and $\nabla_a W_{ab}$

is the weight of the forces depended on the distance and the direction of the separation between particles a and b given by

$$\nabla_a W_{ab} = \begin{cases} -\frac{1}{2h} [(2-q)^2 - 4(1-q)^2] \frac{\mathbf{r}_a - \mathbf{r}_b}{|\mathbf{r}_a - \mathbf{r}_b|}, & 0 \leq q \leq 1 \\ -\frac{1}{2h} (2-q)^2 \frac{\mathbf{r}_a - \mathbf{r}_b}{|\mathbf{r}_a - \mathbf{r}_b|}, & 1 \leq q \leq 2 \\ 0, & 2 < q \end{cases} \quad (9)$$

where $q = |\mathbf{r}_a - \mathbf{r}_b|/h$.

The radius of the support of this W_{ab} is $2h$. If these correspondences are adopted, $2h$ corresponds to the longest distance between lumps a and b at which they interact with each other and is the typical diameter of volume V_a or $2h = \sqrt[3]{V_a}$. It means that the size of the lump corresponds to the radius of the kernel support in the conventional SPH formulation. The resistance force \mathbf{T}_w from the nearby solid surface is the tangential force in the direction opposite of the particle velocity. If \mathbf{t} is the unit vector in the local flow direction, it is expressed as

$$\mathbf{T}_w = -C_T \frac{\tau_w}{h_w} \mathbf{t} \quad (10)$$

where $C_T (=1.0)$ is an empirical constant h_w is the thickness of the wall layer (taken as $2h$) next to the solid boundary and τ_w is the wall shear stress determined by the wall law

$$\frac{v_t}{u_\tau} = \begin{cases} A \ln \left(\frac{nu_\tau}{\nu} \right) + B, & 30 < \frac{nu_\tau}{\nu}, \\ C \ln \left(\frac{nu_\tau}{\nu} \right) + D, & 5 < \frac{nu_\tau}{\nu} < 30, \\ \frac{nu_\tau}{\nu}, & \frac{nu_\tau}{\nu} < 5 \end{cases} \quad (11)$$

where v_t is the tangential velocity of particle a , n is the normal distance from particle a to the boundary, $u_\tau = \sqrt{\tau_w/\rho_a}$, $A(=2.5), B(=5.5), C(=5.0)$ and $D(=3.05)$ are constants and $\nu = \mu_a/\rho_a$, for hydraulically smooth surface with the roughness Reynolds number $R_k = ku_\tau/\nu < 100$ where k is the roughness height. For hydraulically rough surface with $R_k > 100$, the wall law for fully rough surface

$$\frac{v_t}{u_\tau} = A \ln \left(\frac{n}{k} \right) + E \quad (12)$$

with $E=8.5$ is used.

The density is assumed to determine the pressure via a state equation

$$p_a = B \left(\left(\frac{\rho_a}{\rho_0} \right)^\gamma - 1 \right) \quad (13)$$

with the value of B is chosen so that the speed of sound is 10 times the maximum expected flow velocity at the reference density ρ_0 at the atmospheric pressure and $\gamma=7$.

After the velocity \mathbf{v}_a is solved the position \mathbf{r}_a is determined by

$$\frac{d\mathbf{r}_a}{dt} = \mathbf{v}_a \quad (14)$$

which completes the basic equations.

The boundary conditions are the zero normal velocity on solid surface except for infiltration. Rather than introducing artificial repulsive force, the normal velocity component is set to zero when the particle comes within the distance h_w from the boundary. The distance to the boundary is obtained by searching for the closest boundary particle which has the information of position and the normal direction as well as the roughness height and the infiltration capacity. The enforced normal velocity in the wall layer goes in the continuity equation (12) and to automatically increase the density and hence the pressure.

2.2 Representation of rainfall

The rainfall is modelled in the same way as our previous work^{15,16)}, and additional lumps or particles falling on the ground are placed slightly above the ground and above possible water on it. In the 2-d SPH approach of Vacondio et al.¹¹⁾ and Chang et al.⁹⁾ in which the water is represented by columns, particles cannot be added and the mass of columns of water is added according to the precipitation. In 2-d SWE models, rain may be added on grids (RoG)⁴⁾ but since the added rain is very thin and causes wet/dry interface problems⁴⁾. The real rain particles are as small as millimeters in diameter but in the present approach, finite number of lumps that represent some volume of water are introduced at positions separated by distances much larger than the smoothing SPH distance so that they do not interact each other until they come close on the ground. Also, they are introduced at time intervals such that the amount of volume represented by the rain particles in unit time corresponds to the rainfall intensity. The positions where the discrete number of rain lumps or particles are placed are shifted so that the entire catchment receives the rainfall uniformly over the period of the duration of the simulated rainfall.

2.3 Representation of ground and buildings

In the present method the ground and all solid boundaries that may include buildings and structures are defined by a set of discrete particles placed on the solid surfaces. These boundary particles define the position \mathbf{r}_w and the normal direction \mathbf{n}_w of the part of the surface they represent (Fig.4), so that for a water particle that comes close to one of them, the boundary conditions are imposed. The boundary particle that is closest to a water particle is searched by the link-cell method. The ground particles also possess additional information of the ground roughness and the moisture content. The roughness is given in terms of the roughness height k used in the wall law defining the wall stress.

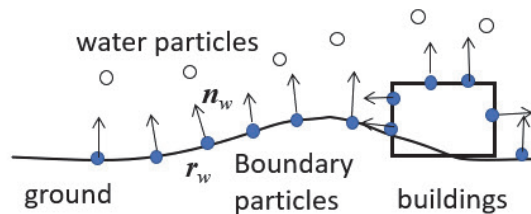


Fig.4 Ground and building surfaces defined by boundary particles placed on the surfaces with the normal direction.

3. SIMULATION OF RAIN RUNOFF FROM MODEL URBAN CATCHMENT

3.1 Model terrain and building array

The present rainfall-runoff simulation is applied to the rainfall runoff simulation from a model urban terrain for which Cea et al.¹⁷⁾ conducted an experiment with a rainfall generator. Fig.5 shows the terrain used in Cea et al experiment and the terrain represented by the boundary particles. Fig. 6 is the configuration S20 in which 20 buildings with sloped roofs are placed in a staggered array. To model the terrain and the buildings in the present method, the total of 107,500 boundary particles placed at the spacing of 0.012m are used. Cea et al.¹⁷⁾ measured the runoff discharge at the lowest boundary ($x=2.5\text{m}$) of the model which can be compared with the present simulation. They also conducted a simulation using the diffusive wave approximation of the SWE, which can also be compared with the present simulation result. They used the building block and building hole models to represent the effects of the buildings but the rain falling on the roof could not be accounted.

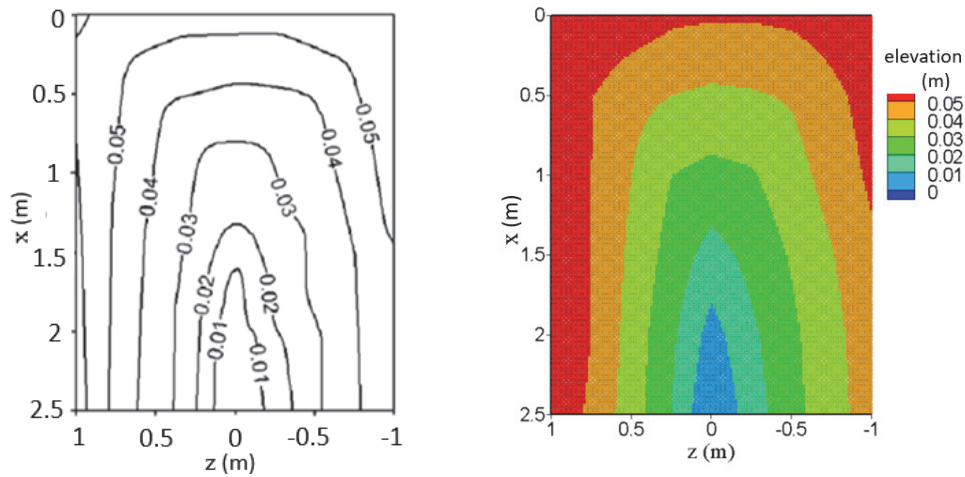


Fig.5 Model terrain of Cea et al.¹⁷⁾ experiment and the present model by boundary particles

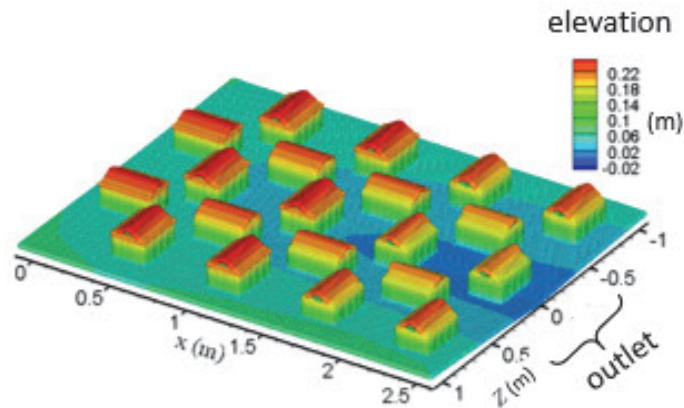


Fig.6 Urban terrain with building configuration S20 of Cea et al.¹⁷⁾ experiment. The terrain and the buildings are represented by boundary particles placed at 0.012m spacing.

3.2 Simulation results

Fig. 7 shows the instantaneous distribution of the rain water at time $t=6$ s and 20 s after it started to rain. The water lump size is 0.012m and the lumps are shown as black dots. The rain intensity is 300mm/h for the period of 40s, which is modelled by placing 100 rain lumps at every 0.4 seconds. The distribution of water is sparse and not quite connected at the beginning $t=6$ s. At $t=20$ s the rain water starts to pond at the higher elevation sides of the buildings. It is noted that more rain water is seen around the buildings than away from the buildings indicating that the rain falling on the sloped roofs slides down the roof dropping around the buildings. The experimental view is not available but they are quite reasonable.

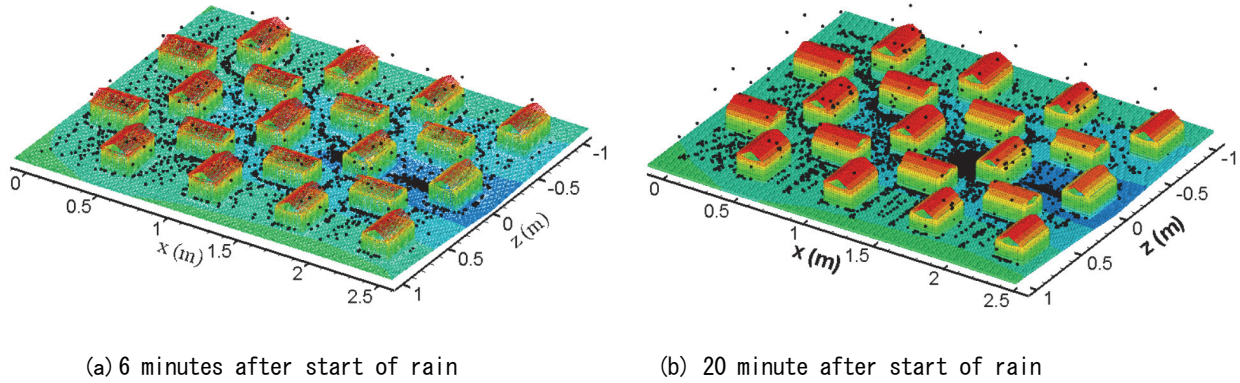


Fig. 7 Simulation results at 2 instances after start of rain. Black dots represent rain water lumps.

The runoff discharge hydrograph obtained from the simulation by counting the rain water flowing out of the downstream end at $x=2.5$ m. The results are compared with the Cea et al.¹⁷⁾ measurements in Fig. 8. Since the material of the model is steel with some rust (Cea et al.¹⁷⁾) the roughness height used in the simulation is 0.5mm everywhere on the ground and the building surfaces. The simulated hydrograph appears faster outflow than the experiment and that the discharge tends to fluctuate. The fluctuation is inevitable in the present discrete particle simulation where the outflow discharge is obtained by counting the number of rain lumps coming out of the outflow section compared with conventional method which calculates the continuously varying average flow velocity and the depth. The fluctuation decreases as the lump size is reduced and the number of lumps is increased. The computational time of simulation over 40 seconds with the present size of water lumps is about 200 hours on a single 3.8GHz CPU computer. The investigation of the resolution effects should be done with a GPU computer in the future work. In the experiments the outflow discharge in the experiments is collected at the center of the lowest side with a collecting channel and there may have been a slight delay. Considering this delay, the obtained hydrograph is reasonable.

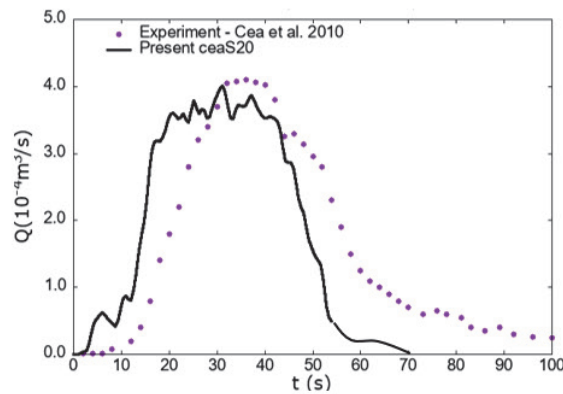
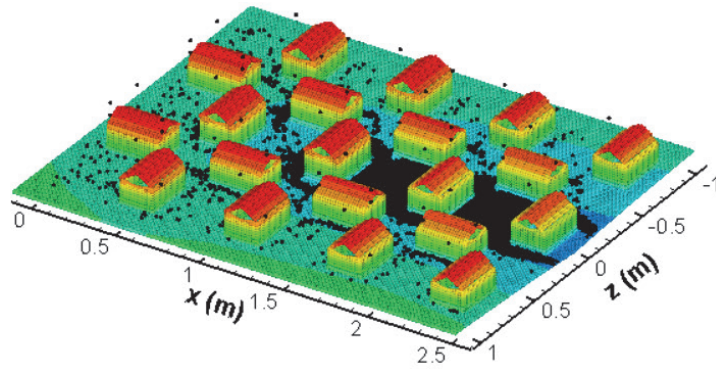


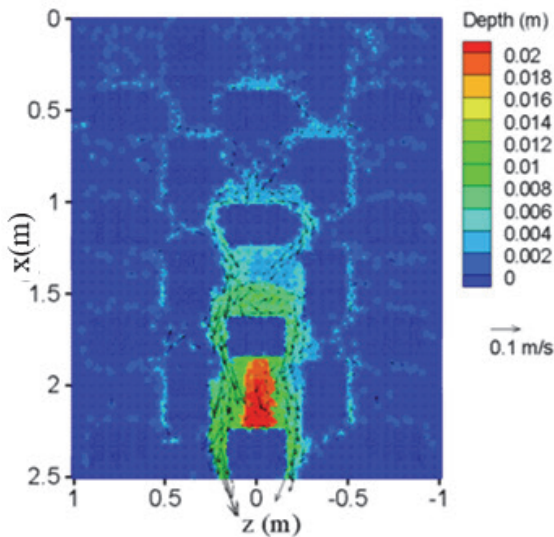
Fig. 8 Discharge hydrograph obtained by the simulation compared with the measurements.

Fig. 9 presents the simulation results at the end of the 40s rainfall. It also compares the present simulation results of the water depth (H) and the depth averaged velocity distributions with the SWE diffusive wave simulation obtained by Cea et al.¹⁷⁾.

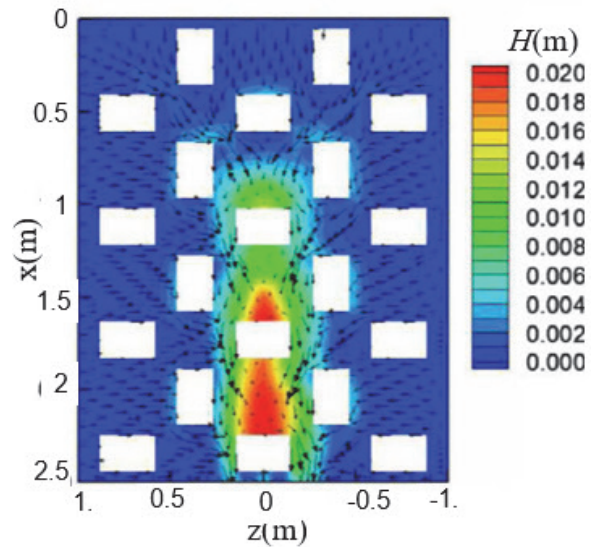
The water depth and the depth-averaged velocity are computed by post-processing the distributed lumps with flow variables. To do it the particle interpolation is applied on the 3-d results at specified 2-d grid points. The color in both plots (a) and (b) indicate the depth with the same color grade scale. They compare fairly well over all but there are some differences. First the water depth of the present result in the ponded area on the higher elevation side of the second building from the outflow section is shallower than Cea et al.¹⁷⁾ calculation. Second, the present results show non-negligible depth around each building while there is no appreciable depth is seen in Cea et al. results. This is the area where the rain falling on the roof drains. Cea et al.¹⁷⁾ does indicate that the building block model does not account for the rain falling on the roofs. The rain draining from the roofs does contribute to the runoff if the roof area is a large and it is accounted for in the present SPH simulation.



(a) The rain water distribution at $t=40s$



(b) The simulated depth distribution at $t=40s$



(c) Simulation by Cea et al.¹⁷⁾

Fig. 9 Comparison of the distribution of the depth and the depth averaged flow velocity with the SWE simulation of Cea et al.¹⁷⁾.

4. CONCLUSION

The weakly compressible smoothed particle hydrodynamics (WCSPH) has been re-derived from the integral forms of conservation laws so that the resulting equations can be used for the motion of thinly dispersed overland flow with three-dimensional topographic effects of buildings in urban catchment. The equations for the motion of finite lumps of water were derived. The resulting equations are similar to the conventional SPH equations but they indicate that the force terms are interpreted as the interactions with neighboring fluid and solid boundaries. The latter interaction, particularly, allowed imposition of laminar or turbulent wall-laws to be implemented near the ground or other surfaces avoiding complex treatment used in conventional methods.

Also, the method is quite effective in representing the sparsely distributed complex flow on three-dimensional topography. The rain water flow falling on the terrain and on buildings can be represented well without the commonly encountered wet/dry boundary problems. The depth of water is not the direct variable that is solved and it needs to be analyzed from the distribution of discrete lumps using a separate model. The presently obtained results of inundation depth is very reasonable.

The simulation of the overland flow and the inundation in a model urban terrain with three-dimensional effects due to buildings gave promising results compared with the existing methods. The method can further be applied to simulation of more general rain-runoff simulation.

ACKNOWLEDGEMENT

The present work was partly supported by Universiti Tunku Abdul Rahman Research Fund UTARRF/2022-C1/A03 and Malaysian Ministry of Higher Education Fundamental Research Grant System FRGS/1/2019/TK01/UTAR/01/1.

REFERENCES

- 1) Zhang, W. and Cundy, T. W.: Modeling of two-dimensional overland flow, *Water Resources Research*, Vol. 25, pp. 2019-2035, 1989.
- 2) Teng, J., Jakeman, A., Vaze, J., Croke, B. F., Dutta, D. and Kim, S.: Flood inundation modelling: A review of methods, recent advances and uncertainty analysis, *J. Hydrol.*, Vol.315, 220-235, 2005.
- 3) Li, X., Fang, X., Li, J., Manoj, K.C., Gong, Y. and Chen, G.: Estimating time of concentration for overland flow on pervious surfaces by particle tracking method, *Water MDPI*, Vol. 10, 379, 2018.
- 4) Constabile, P., Constanzo, C., Ferraro, D. and Barca, P.: Is HEC-RAS 2D accurate enough for storm-event hazard assessment? Lessons learnt from a benchmarking study based on rain-on-grid modelling, *J. Hydrol*, Vol.603 (B) 126962, 2021.
- 5) Sayama, T., Yamada, M., Sugawara, Y., Konja, A., Sekimoto, T. and Yamazaki, D.: Flood inundation simulation using a large-scale rainfall runoff-inundation model – effects of topographic data corrections-, *Journal of Japan Society of Civil Engineers, Ser. B1(Hydraulic Engineering)*, Vol. 78, No.2, I_565-I_570, 2022.
- 6) Sitterson, J., Knightes, C., Parmar, R., Wolfe, K., Muche, M. and Avant, B.: An overview of rainfall-runoff model types. Athens: Unites States Environmental Protection Agency, 2017.
- 7) Gayathri, K.D., Ganasri, B.P., and Dwarakish, G.S.: A Review on Hydrological Models, *Aquatic Procedia*, 4, pp.1001–1007. <http://dx.doi.org/10.1016/j.aqpro.2015.02.126>, 2015.
- 8) Kokkonen, T., Koivusalo, H. and Karvonen, T.: A semi-distributed approach to rainfall-runoff modelling—a case study in a snow affected catchment. *Environmental Modelling & Software*, 16(5), pp.481-493, 2001.
- 9) Chang, T.-J., Chang, Y.-S. and Chang, K.-H.: Modeling rainfall-runoff processes using smoothed particle hydrodynamics with mass-

- varied particles, *J. Hydrol.*, Vol. 543, pp. 749-758, 2016.
- 10) Fei, X., Yan, H., Tao, T., Xin, K. and Li, S.: Integrated rainfall-runoff process with shallow water model by mass varied smoothed particle hydrodynamics: Infiltration effect implementation, *J. Hydrodynam.*, Vol. 33, pp.1190-1201, 2021.
 - 11) Vacondio R., Rogers B. D., Stansby, P. K.: SPH modeling of shallow flow with open boundaries for practical flood simulation, *J. Hydraul. Eng.*, Vol. 138(6), pp. 530–541, 2012.
 - 12) Monaghan, J. J. : Simulating free surface flows with SPH, *J. Comput. Phys.* Vol. 110. pp. 399-406, 1994.
 - 13) Violeau, D. and Rogers, B. D.: Smoothed particle hydrodynamics (SPH) for free-surface flows: past, present and future, *J. Hydraul. Res.*, Vol. 54, No. 1, pp. 1-26, 2016.
 - 14) Nakayama, A., Lye, X.Y. and Ng, K.C.: Wall-layer boundary condition method for laminar and turbulent flows in weakly compressible SPH, *Eur. J. of Mech. /B Fluids*, Vol. 95, pp. 276-288, 2022.
 - 15) Tan, S.Y, Nakayama, A. and Lye, X.Y. : Application of particle method to simulation of runoff from short but intense rainfall and street flooding in s small catchment, *Memoir of Construction Engineering Research Institute* Vol..64, pp.1-11, 2022.
 - 16) Lye, X.Y., Nakayama, A. and Tan, S.Y.: Simulation of overland flow due to rainfall using smoothed particle hydrodynamics, *Journal of Japan Society of Civil Engineers Ser B (Hydraulic Engineering)*, Vol.78, No.2,I_553-I_558, 2022.
 - 17) Cea, I., Garrido, M. and Puertas, J. :Experimental validation of two-dimensional depth-averaged models for forecasting rainfall-runoff from precipitation data in urban areas, *J. Hydrol.*, Vol.382, pp.88-102, 2010.

AUTHORS

Akihiko Nakayama Ph D., Fluid Mechanics, Hydraulics, Universiti Tunku Abdul Rahman, Malaysia

Lye Xin Yan, Environmental Engineering, Graduate student B.S., Universiti Tunku Abdul Rahman, Malaysia